

Figure 1. Structures of the FeGP cofactor and its light decomposition product (iron-free FeGP cofactor). The FeGP cofactor binds to [Fe]-hydrogenase with the sulfur of a conserved cysteine. The FeGP cofactor can be reversibly extracted from the protein by denaturation in the presence of acetic acid or 2-mercaptoethanol. The proposed structures of the extracted cofactors are shown. The FeGP cofactor form detected by ESI-MS is generated from the extracted forms during electrospray ionization.¹⁰ The individual carbons of the iron-free FeGP cofactor were labeled with stable isotopes as shown in the figure.

Pyridinol/pyridone derivatives in the form of pyridone polyketides are ubiquitous among alkaloids produced in plants, fungi, and actinomycetes;¹¹ however, such a highly substituted pyridinol ring structure as found in the FeGP cofactor is rare. All of the substituents of the pyridinol ring of the FeGP cofactor should play crucial roles in its function. Crystal structure analyses have indicated that the guanosine monophosphate

moiety of FeGP cofactor binds to the nucleotide monophosphate binding site on the N-terminal Rossmann-fold domain of this enzyme.¹² The electron-donating methyl groups of this ring system. Furthermore, density functional theory (DFT) calculations indicated that the hydroxyl group of the pyridinol moiety could be involved in the catalytic reactions.¹³ In addition, the strong *trans*-influencing character of the acyl ligand¹⁴ is considered to play an important role for hydrogen activation because the iron site *trans* to the acyl ligand is proposed to be a H_2 -binding site.⁵

In this study, we carried out *in vivo* labeling experiments with ^{13}C - and ^2H -labeled precursors to obtain first insights into how the FeGP cofactor might be synthesized. For these experiments, *Methanothermobacter marburgensis* and *Methanobrevibacter smithii* were selected. *Mt. marburgensis* grows autotrophically on H_2/CO_2 up to very high cell densities and overproduces [Fe]-hydrogenase under nickel-limiting conditions up to 7% of the soluble proteins,¹⁵ allowing us to obtain micromole amounts of labeled cofactor. Despite the autotrophic growth, the organism does assimilate acetate, pyruvate, and methionine when added to the growth medium,¹⁶ albeit only low amounts, resulting in partially isotope-labeled cell components. The partial labeling and the amounts of cofactor obtained were, however, sufficient for the determination of the labeling pattern via NMR. *Mb. smithii*, the second organism used, is not an autotroph;¹⁷ it requires exogenous acetate as a carbon source in addition to CO_2 because it lacks the nickel-dependent CO dehydrogenase and therefore cannot synthesize acetyl-coenzyme A (acetyl-S-CoA) from 2CO_2 . Consequently, in *Mb. smithii*, the cell components derived from acetate are in principle fully enriched with the label of ^{13}C -labeled acetate added to the medium. However, *Mb. smithii* grows poorly and contains relatively low amounts of [Fe]-hydrogenase. Therefore, the FeGP cofactor labeled in *Mb. smithii* could only be analyzed by mass spectrometry rather than by NMR.

RESULTS

Mt. marburgensis and *Mb. smithii* were grown on H_2 and CO_2 in media supplemented with ^{13}C - or ^2H -labeled putative precursors in FeGP cofactor biosynthesis. The position of incorporated ^{13}C and ^2H stable isotopes in the iron-free FeGP cofactor was analyzed by NMR and the number of ^{13}C isotopes incorporated was analyzed by mass spectrometry. NMR analysis was only possible with the iron-free FeGP cofactor because of line broadening caused by high-spin $\text{Fe}^{\text{II/III}}$ released upon decomposition of the FeGP cofactor. During MALDI-TOF-MS analysis a decarboxylated derivative of the iron-free cofactor was generated whose labeling was also analyzed.

In methanogens, pyruvate is synthesized from acetyl-S-CoA via reductive carboxylation. C-2 and C-3 of pyruvate are therefore derived from C-1 and C-2 of acetate, respectively, and C-1 of pyruvate is derived from CO_2 . Therefore, labeling experiments with ^{13}C from $[\text{1-}^{13}\text{C}]$ acetate, $[\text{2-}^{13}\text{C}]$ acetate, $[\text{1-}^{13}\text{C}]$ pyruvate, and $^{13}\text{CO}_2$ complement each other.

Acetate, pyruvate, methionine, glycine, formate, CO_2 , and CO were found to be incorporated into the FeGP cofactor by growing *Mt. marburgensis* or *Mb. smithii*. The degree of labeling in *Mt. marburgensis* was 20% in the case of acetate (5 mM), <10% in the case of pyruvate (7 mM), 80% in the case of methionine (5 mM), and 90% in the case of formate (40 mM).

Labeling with glycine (19%) was only possible in *Mb. smithii* because *Mt. marburgensis* is not capable of taking up glycine. The degree of labeling of the cofactor in *Mb. smithii* was around 90% in the case of CO₂ and 80% in the case of CO. The enrichment was estimated by NMR or MALDI-TOF-MS of the iron-free FeGP cofactor.

Carbon Atoms Derived from [1-¹³C]Acetate. The ¹³C NMR spectrum of iron-free FeGP cofactor labeled with ¹³C from [1-¹³C]acetate in *Mt. marburgensis* showed six ¹³C-enriched peaks, which corresponded to C(b), C(f), and C(e) of the pyridinol, C(1') and C(4') of the ribose, and C(5) of guanine, based on the chemical shift data reported previously (Table 1; Figure S1, Supporting Information).¹⁸ ¹H-¹³C

Table 1. ¹³C-Chemical Shifts of the Iron-Free FeGP Cofactor from *Mt. marburgensis* Cultivated with ¹³C-Labeled Substrates in D₂O at 300 K

position	chemical shift of the observed ¹³ C NMR peak ^a		
	[1- ¹³ C]acetate	[2- ¹³ C]acetate	[1- ¹³ C]pyruvate ^c
	pyridinol		
b	167.3		
c			120
d			163
e	116.2		
f	140.2		
g		38.1	
i ^b		13.2	
	Ribose		
1'	90.2		
2'			76
3'			73
4'	86.4		
5'		68.3	
	Guanine		
4			154
5	118.1		

^aChemical shifts of the nonlabeled carbons are not shown (See Figure S1, Supporting Information). ^bRevised assignment, see text for details. ^cChemical shifts without calibration with 4,4-dimethyl-4-silapentane sodium sulfonate.

heteronuclear multiple-bond correlation (HMBC) indicated strong correlations between H(j) and C(b), H(i) and C(e), and H(i) and C(f) (Figure 2A), while ¹H-¹³C heteronuclear single-quantum correlation (HSQC) showed strong peaks between H(1') and C(1'), and H(4') and C(4'), which corroborated the assignments of the labeled carbons (spectrum not shown).

The NMR results were confirmed by MALDI-TOF-MS (positive mode) performed with the FeGP cofactor labeled in *Mb. smithii*. The analysis revealed the incorporation of six ¹³C from [1-¹³C]acetate into the iron-free FeGP cofactor and six ¹³C into decarboxylated cofactor generated during laser ionization (Figure 3).^{10,18} Their corresponding mass peaks were observed at *m/z* 549 and at *m/z* 505, respectively (Figure 3B left). The presence of the multiple isotopic peaks indicated that the ¹³C enrichment in the FeGP cofactor was about 80% (Figure S4, Supporting Information). We attributed this to the salvage biosynthesis of GMP in *Mb. smithii*, which uses exogenous guanine from yeast extract added to the medium (2 g/L), as previously described by Choquet et al.¹⁹ Consistently, the enrichment increased to almost 90% when *Mb. smithii* was grown on media supplemented with only 0.05 g/L yeast extract.

MS/MS revealed that the pyridinol moiety contained three ¹³C, which were almost 100% derived from [1-¹³C]acetate (Table 2). Via MS/MS, it was also observed that two ¹³C were incorporated into the ribose moiety and one ¹³C into the purine ring (summarized in Table 2).

Carbon Atoms Derived from [2-¹³C]Acetate. ¹³C NMR analysis of the iron-free FeGP cofactor labeled with ¹³C from [2-¹³C]acetate in *Mt. marburgensis* revealed three intense peaks at 13.2, 38.1, and 67.9 ppm. The three peaks were assigned as C(i), C(g), and C(5') from the ¹³C-chemical shifts (Table 1 and Figure S1, Supporting Information) and the ¹H-¹³C HSQC spectrum (Figure 2B). The 38.1 ppm C(g) peak was relatively small and was line broadened. Such line broadening of the C(g) peak has also been observed in our earlier study.¹⁸ The reason appears to be the partial exchange of the hydrogen atoms at this carbon with ²H₂O. Based on our published ¹³C NMR shift data, the 13.2 ppm peak had been assigned as C(j), which is one of the two methyl groups of the pyridinol ring.¹⁸ Because the earlier assignment did not fit to the ¹H-¹³C HMBC and HSQC data in this study, the ¹³C chemical shifts of C(j) and C(i) were reassigned as follows. ¹H-¹³C HSQC analysis revealed that the carbon with $\delta = 13.2$ ppm connects to proton at 1.78 ppm, which was assigned as H(i) by the published data, and it was confirmed as described below. The ¹H signal of H(i) shows enhanced ¹³C-satellites due to partial ¹³C enrichment on this position (Figure 2B, ¹H projection). Integral of the ¹H signals revealed an enrichment rate of 18%. The assignment of H(i) was confirmed by ¹H-¹³C HMBC, which indicated connectivity of H(i) with C(d), C(e), and C(f) but not with C(b) and C(c) (Figure S2, Supporting Information). Consequently, the carbon with $\delta = 13.2$ ppm was reassigned as C(i). Accordingly, the carbon with $\delta = 12.4$ ppm was reassigned as C(j). It is important to note that although the ¹³C-chemical shifts of the two methyl carbons were reassigned, the chemical structure of the iron-free FeGP cofactor was not changed.

The NMR results were confirmed by MALDI-TOF-MS performed with the FeGP cofactor labeled in *Mb. smithii*. The analysis revealed that three ¹³C from [2-¹³C]acetate were incorporated into the iron-free FeGP cofactor and its decarboxylated derivative (Figure 3C, left) with an enrichment of about 90% (Figure S4, Supporting Information). MS/MS analysis indicated that two ¹³C were incorporated into the pyridinol moiety and one ¹³C was incorporated into the ribose moiety (Table 2).

Carbon Atoms Derived from [1-¹³C]Pyruvate. Even though the intensity of the ¹³C-enriched NMR peaks of the cofactor labeled with ¹³C from [1-¹³C]pyruvate in *Mt. marburgensis* was lower than the intensity of the ¹³C-enriched NMR peaks of the cofactor labeled with ¹³C from [1-¹³C]acetate and [2-¹³C]acetate, the ¹³C NMR spectrum clearly revealed five ¹³C-enriched peaks at 73, 76, 120, 154, and 163 ppm. These peaks were assigned as C(3'), C(2'), C(c), C(4), and C(d) based on the chemical shifts of the previous report (Figure S1C, Supporting Information).¹⁸ ¹H-¹³C HMBC indicated the correlation between H(j) and C(c), H(j) and C(d), H(1') and C(2'), and H(1') and C(4). Because of the lower enrichment in ¹³C and the lower concentration of the sample, the background peaks were relatively high. However, most of the extra peaks can easily be excluded from the data set because the chemical shifts did not fit to the original data at all.¹⁸ Only the peak observed at 174 ppm was similar to that of C(h) ($\delta = 177.6$ ppm), but ¹H-¹³C HMBC did not show the

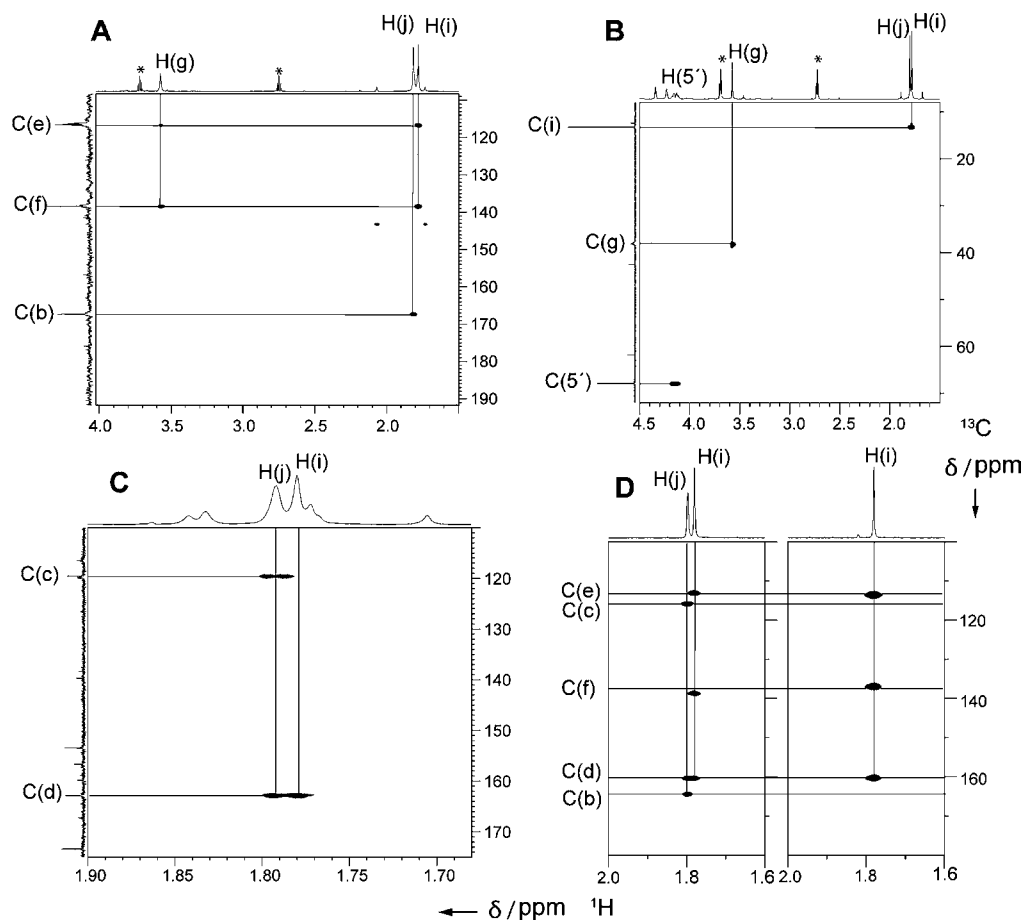


Figure 2. Two-dimensional NMR analyses of the iron-free FeGP cofactor labeled with ^{13}C and ^2H from labeled compounds. The samples were dissolved in $^2\text{H}_2\text{O}$ and measured at 300 K. (A) ^1H - ^{13}C HMBC spectrum of the cofactor labeled with ^{13}C from $[1-^{13}\text{C}]$ acetate. (B) ^1H - ^{13}C HSQC spectrum of the cofactor labeled with ^{13}C from $[2-^{13}\text{C}]$ acetate. Signals arising from contaminants are marked with an asterisk. (C) ^1H - ^{13}C HMBC spectrum of the cofactor labeled with ^{13}C from $[1-^{13}\text{C}]$ pyruvate. The ^1H NMR signals were broadened, most probably by contaminating iron ions. (D) ^1H - ^{13}C HMBC spectrum of the nonlabeled cofactor (left) and the cofactor labeled with ^2H from L -[methyl- ^2H]methionine (right).

cross peak with H(g) (Figure 2C). Therefore, we concluded that C(h) was not enriched with $[1-^{13}\text{C}]$ pyruvate. Thus, ^1H - ^{13}C HMBC unequivocally assigned the positions of the labeled carbons.

The NMR results were confirmed by MALDI-TOF-MS performed with the FeGP cofactor labeled in *Mt. marburgensis*. Mass peaks at m/z 543–548 (+0 to +5) and m/z 499–504 (+0 to +5), respectively, were observed (Figure 3D, left). The analysis revealed that five ^{13}C from $[1-^{13}\text{C}]$ pyruvate were incorporated into the iron-free FeGP cofactor and into its decarboxylation derivative with an enrichment of about 50% (Figure S4, Supporting Information). MS/MS analysis indicated that two ^{13}C from $[1-^{13}\text{C}]$ pyruvate were incorporated into the pyridinol moiety, two into the ribose moiety, and one into the purine moiety (Table 2).

Hydrogen Atoms Derived from L -[Methyl- $^2\text{H}_3$]-methionine. In a preliminary study, we had found that the iron-free FeGP cofactor isolated from *Mt. marburgensis* grown in the presence of L -[methyl- ^{13}C]methionine showed an increase of $m/z = 1$, which indicates that one of the methyl groups on the pyridinol ring originates from L -methionine.²⁰ The ^1H NMR spectrum of the methyl- ^2H -labeled iron-free FeGP cofactor now revealed the methyl group to be attached to C(c) as indicated by a strong decrease in the H(j) peak height

at 1.82 ppm (Figure S3, Supporting Information). ^1H - ^{13}C HMBC indicated that the $^{13}\text{C}/^1\text{H}$ cross peaks at H(j) were not visible, but the H(i) peak at 1.78 ppm reasonably revealed cross peaks with C(d), C(e), and C(f), which showed that the methyl group attached to C(c) was completely deuterated (Figure 2D).

Carbon Atoms from $^{13}\text{CO}_2$. In the MALDI-TOF-MS spectrum of FeGP cofactor labeled with ^{13}C from $^{13}\text{CO}_2$ in *Mb. smithii*, a peak at m/z 553 (+10) (90% enrichment) was detected (Figure 4A left), which indicated that 10 ^{13}C from $^{13}\text{CO}_2$ were incorporated into the iron-free FeGP cofactor (Figure S4, Supporting Information). In case of the decarboxylated form, it was nine carbon atoms (m/z 508) from CO_2 indicating that the C(h) carboxyl group is derived from $^{13}\text{CO}_2$.

Carbon Atoms from $[1-^{13}\text{C}]$ Glycine and $[^{13}\text{C}]$ Formate. MALDI-TOF-MS and MS/MS data indicated that $[1-^{13}\text{C}]$ -glycine was incorporated by *Mb. smithii* exclusively into the purine part of the iron-free FeGP cofactor, which is in agreement with common purine biosynthesis (Table 2).¹⁹ In the $[^{13}\text{C}]$ formate-labeling experiment with *Mt. marburgensis*, one purine carbon was labeled with ^{13}C from $[^{13}\text{C}]$ formate. This result is consistent with the known incorporation of formate into the C(2) of purine.²¹ $[^{13}\text{C}]$ Formate was not incorporated into the pyridinol moiety.

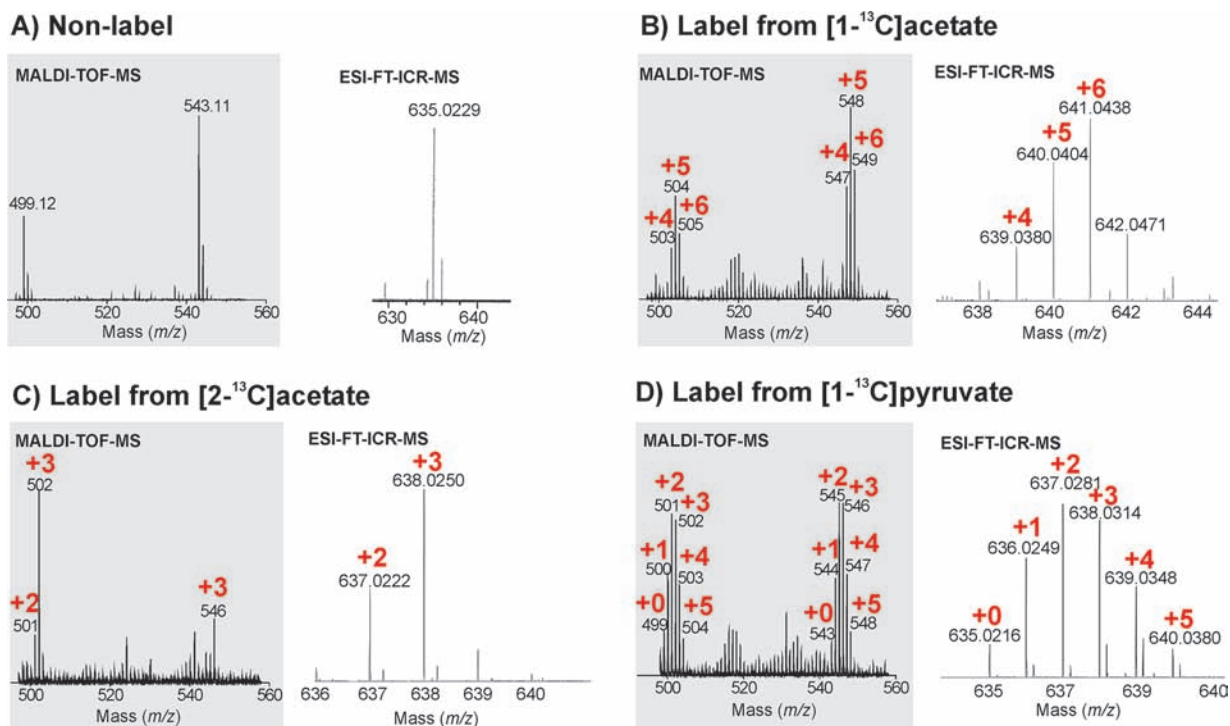


Figure 3. MALDI-TOF-MS and ESI-FT-ICR-MS mass spectra of (A) nonlabeled and (B–D) ^{13}C -labeled FeGP cofactor from *Mb. smithii*. The ^{13}C substrates used for labeling are indicated. The increase of m/z owing to incorporation of ^{13}C is shown in red. In MALDI-TOF-MS spectra, the iron-free cofactor and a decarboxylated derivative were detected. (A, right) The typical ^{54}Fe isotopic peak could not be observed due to the low FeGP cofactor concentration of the sample.¹⁰

Table 2. Incorporation of Stable Isotopes from $[1-^{13}\text{C}]$ Acetate, $[2-^{13}\text{C}]$ Acetate, $^{13}\text{CO}_2$, L-[Methyl- ^2H]methionine, and $[1-^{13}\text{C}]$ Glycine into the FeGP Cofactor of *Mb. smithii* and from $[1-^{13}\text{C}]$ Pyruvate and $[1-^{13}\text{C}]$ Formate into the FeGP Cofactor of *Mt. marburgensis*^a

^{13}C -labeled substrate	number of stable isotopes in the FeGP cofactor parts					
	total ^b	pyridinol ^c	ribose	guanine	CO ligands ^d	acyl ligand ^e
$[1-^{13}\text{C}]$ acetate	6	3	2	1		
$[2-^{13}\text{C}]$ acetate	3	2	1			
$^{13}\text{CO}_2$	12	3	2	4	2	1
^{13}CO	3				2	1
$[1-^{13}\text{C}]$ pyruvate	5	2	2	1		
$[1-^{13}\text{C}]$ formate	1			1		
L-[methyl- ^2H]methionine	1	1			<i>f</i>	
$[1-^{13}\text{C}]$ glycine	1			1	<i>f</i>	
$[1-^{13}\text{C}]$ propionate					<i>f</i>	
$[2,3-^{13}\text{C}_2]$ succinate					<i>f</i>	

^aStable isotopes were detected by MALDI-TOF-MS and MS/MS.

^bTotal carbons of the FeGP cofactor. ^cCarbons of pyridinol other than C(h) that is indicated as acyl ligand.

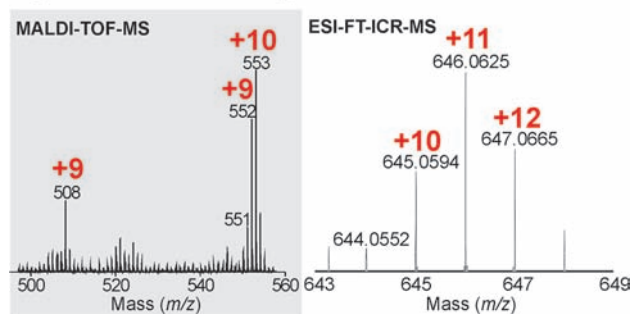
^dDetermined by ESI-FT-ICR-MS.

^eThe number of incorporation of ^{13}C into the carboxyl group C(h).

^fNot tested.

Lack of Labeling of the Iron-Free FeGP Cofactor by $[1-^{13}\text{C}]$ Propionate and $[2,3-^{13}\text{C}]$ Succinate. $[1-^{13}\text{C}]$ -Propionate and $[2,3-^{13}\text{C}]$ succinate were not incorporated into the iron-free FeGP cofactor by *Mt. marburgensis*, although these acids were assimilated into other cell components,¹⁶ for example,

A) Label from $^{13}\text{CO}_2$



B) Label from ^{13}CO

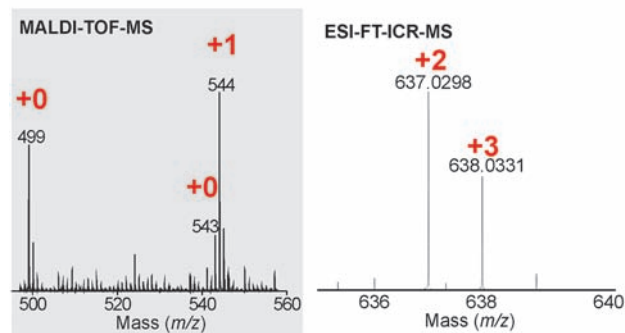


Figure 4. MALDI-TOF-MS and ESI-FT-ICR-MS mass spectra of the FeGP cofactor labeled with ^{13}C from (A) $^{13}\text{CO}_2$ and (B) ^{13}CO . The increase in m/z owing to the incorporation of ^{13}C is shown in red.

propionate into isoleucine and succinate into F_{430} as revealed by mass spectrometry (Figures S5 and S6, Supporting Information).

Labeling of the CO- and Acyl Ligands in the FeGP Cofactor. As indicated above, the complete FeGP cofactor could not be analyzed by NMR because of line broadening due to high-spin iron contaminations nor by MALDI-TOF because of decomposition of the FeGP cofactor by irradiation with the laser. Therefore, the following analyses were performed by ESI-FT-ICR-MS and ATR-IR, which allowed detection of the complete FeGP cofactor.

The labeling experiments with $[1-^{13}\text{C}]$ acetate, $[2-^{13}\text{C}]$ acetate (*Mb. smithii*), and $[1-^{13}\text{C}]$ pyruvate (*Mt. marburgensis*) revealed the FeGP cofactor and the iron-free FeGP cofactor to have the same mass increases (Figure 3B–D) indicating that the CO ligands are not biosynthetically derived from these precursors. When CO_2 was the labeled precursor (*Mb. smithii*) the complete FeGP cofactor showed a mass increase of 12 (Figure 4A, right), whereas the iron-free FeGP cofactor determined by MALDI-TOF-MS showed a mass increase of only 10 (Figure 4A, left, $m/z = 553$). The decarboxylated form showed a mass increase of nine (Figure 4A, left, $m/z = 508$). These findings indicate that the two CO and the acyl group are biosynthetically derived from CO_2 . With CO as the ^{13}C -labeled precursor (*Mb. smithii*) the complete FeGP cofactor showed a maximal mass increase of three (Figure 4B, right) (^{13}C enrichment 70%, see detailed analysis in the legend of Figure S4, Supporting Information), whereas the iron-free FeGP cofactor determined by MALDI-TOF-MS showed a maximal mass increase of one (Figure 4B, left, $m/z = 544$) (80%). The decarboxylated form showed no mass increase (Figure 4B, left, $m/z = 499$). These findings indicate that the two CO and the acyl group are derived from CO when added to the cultures. ^{13}C from formate was not incorporated in one of the iron ligands (Table 2).

Infrared Spectrum of FeGP cofactor Labeled with ^{13}CO . To determine the incorporation of ^{13}CO into the CO ligands of the FeGP cofactor, we analyzed [Fe]-hydrogenase by ATR-IR spectroscopy. To obtain large amounts of [Fe]-hydrogenase, *Mt. marburgensis* was used for the experiment. With the nonlabeled enzyme, peaks at 2009 and 1942 cm^{-1} were observed, which correspond to asymmetric and symmetric coupling vibrations of two CO bound to the iron in *cis* orientation, respectively (Figure 5).⁷ With the enzyme labeled

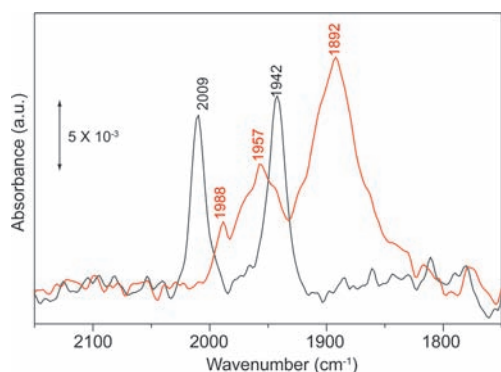


Figure 5. Attenuated total reflection infrared spectra of the partially purified [Fe]-hydrogenase preparation showing the CO ligand region of the FeGP cofactor. Black line, the nonlabeled FeGP cofactor; red line, FeGP cofactor labeled with ^{13}C from ^{13}CO .

with ^{13}CO , the two CO frequencies were shifted to 1957 and 1892 cm^{-1} and broadened. The major peaks appear to correspond to the CO ligands fully exchanged by ^{13}CO , and the shoulders at 1988 and ~ 1900 cm^{-1} appear to be those of

only one of the two *cis* CO ligands exchanged by ^{13}CO . The authentic CO frequency at 2009 cm^{-1} was not visible in the spectrum of the ^{13}CO -labeled sample, which indicated that at least one CO ligand of the individual iron site was fully exchanged. Because of the very large amide peak at ~ 1600 cm^{-1} , the acyl–iron ligand peak (~ 1700 cm^{-1}) was not visible; therefore, we could not determine the labeling of the acyl ligand by ^{13}CO .

DISCUSSION

The FeGP cofactor contains 21 carbon atoms, 5 in the guanine moiety, 5 in the ribose moiety, 9 in the pyridinol moiety, and 2 in the two CO ligands. In *Mt. marburgensis* growing autotrophically on H_2 and CO_2 , all 21 C atoms are derived from CO_2 . The number of carbon atoms derived exclusively from CO_2 decreased to 12 when the growth medium was supplemented with acetate. In *Mb. smithii*, which is dependent on acetate for growth, always 12 carbon atoms are derived from CO_2 and 9 carbon atoms from acetate: 6 from C-1 of acetate and 3 from C-2 of acetate. This is the result of the labeling experiments with $[1-^{13}\text{C}]$ acetate, $[2-^{13}\text{C}]$ acetate, and $^{13}\text{CO}_2$ reported above. The carbon atoms derived from the labeled precursors are shown in Figure 1.

In the two methanogens, acetate is assimilated via activation to acetyl-CoA, which is either condensed to acetoacetyl-CoA, from which the isoprenoid membrane lipids are synthesized, or reductively carboxylated to pyruvate, from which almost all other cell components are generated. Labeling studies with $[1-^{13}\text{C}]$ pyruvate revealed that 5 of the 21 C-atoms in the FeGP-cofactor are derived from C-1 of pyruvate, one less than from C-1 of acetate. This finding indicates that either one acetate is incorporated into the FeGP cofactor without pyruvate being an intermediate or one pyruvate is incorporated into the cofactor losing C-1 on the way.

The observation that six C-atoms are derived from C-1 of acetate and only three C atoms from C-2 of acetate can be explained by two findings: (i) Two of the 21 C-atoms of the FeGP cofactor at the purine moiety are derived from glycine, which in methanogens is synthesized from C-1 and C-2 of pyruvate via 3-hydroxypyruvate and serine, C-3 of serine (=C-3 of pyruvate = C-2 of acetate) yielding methylene- H_4MPT , which is reduced to methane;²² (ii) The labeling pattern of the pyridinol ring of the iron-free FeGP cofactor at C(i), C(e), C(d), C(c), and C(b) is identical to that of the ribose moiety indicating the involvement of two pentoses in the biosynthesis of the FeGP cofactor.²³ Pentoses in methanogens are synthesized from hexulose-6-phosphate, C-1 of the hexulose (=C-3 of pyruvate = C-2 of acetate) yielding methylene- H_4MPT , which is reduced to methane.²⁴ The hexulose phosphate is synthesized from pyruvate via reversal of the Embden–Meyerhof pathway as indicated by the finding that both in the ribose moiety and the pyridinol moiety two neighboring carbon atoms are derived from C-1 of pyruvate.

When *Mt. marburgensis* was grown in the presence of methionine, the FeGP cofactor contained only 20 carbon atoms from CO_2 and 1 C atom from the methyl group of methionine, which in methanogens is synthesized from CO_2 via methyl- H_4MPT , the methyl group of the latter being transferred to homocysteine.²⁵ The methyl group of methionine was incorporated intact into the C(j) position of the pyridinol moiety as revealed by MS and NMR analysis of the L-[methyl- $^2\text{H}_3$]methionine-labeled cofactor indicating that methyl transfer from methionine is catalyzed by a

SAM-dependent methyltransferase rather than by a radical SAM enzyme.^{26,27}

This leaves six C atoms in the FeGP cofactor not derived from C-1 and C-2 of acetate, C-1 of pyruvate, or the methyl group of methionine. Three of the six carbons are attributed to three carbon atoms in the purine ring, which are synthesized from CO₂ (one via formate).^{19,21} The other three carbon atoms are those of the two CO- and the one acyl-ligands to iron in the cofactor. Labeling experiments with ¹³CO₂ showed that the three ligands are derived from CO₂ and labeling experiments with acetate and pyruvate that pyruvate is not an intermediate in their biosynthesis. The latter finding excludes dehydroglycine as an intermediate, which was recently shown to be the precursor of the CO ligands to iron in [FeFe]-hydrogenases.^{28,29} Dehydroglycine is generated from *p*-hydroxyphenylalanine (tyrosine) in a radical SAM reaction yielding *p*-cresol as second product, the two C-atoms in dehydroglycine being derived from C-1 and C-2 of tyrosine (=C-1 and C-2 of pyruvate). In the case of [NiFe]-hydrogenase, glycerol has been shown to be an intermediate in CO-ligand biosynthesis in *Ralstonia eutropha* when grown under heterotrophic growth conditions.³⁰ In methanogens, glycerol is generated from pyruvate, which has been shown not to be an intermediate in CO-ligands biosynthesis of [Fe]-hydrogenase. The findings show that the biosynthesis of the

CO ligands to iron in the FeGP cofactor is different from that in both [FeFe]- and [NiFe]-hydrogenases.^{28–30}

When *Mb. smithii* was grown in the presence of ¹³CO, the three carbon-containing ligands became labeled. However, the results cannot be interpreted to indicate that CO₂ is incorporated into the three iron ligands via free CO since *Mb. smithii* lacks the only enzyme known to catalyze the reduction of CO₂ to CO, namely a nickel-dependent CO dehydrogenase.¹⁷ Incorporation of CO was thus probably via a salvage pathway although it cannot be excluded that *Mb. smithii* contains a noncanonical CO dehydrogenase not yet identified. Labeling of the acyl carbon by ¹³CO could occur by scrambling of the CO- and acyl ligands, as observed in model compounds irradiated by light.^{31,32} How the unique acyl iron bond is formed remains elusive. The formation of the acetyl-nickel bond from acetyl-CoA in the acetyl-CoA synthase/decarbonylase of acetogens and methanogens could stand as model.^{33,34}

Based on these results, several biosynthetic pathways can be thought of following the retrosynthesis concept in organic chemistry described by Eisenreich and Bacher.³⁵ Each of these pathways has a few unknowns. The pathway shown in Figure 6 assumes that the 2,3-dihydroxy-4-oxo-pentanoate and aspartate condense to yield the pyridinol moiety most probably with a pyridoxal phosphate bound β -alanine as intermediate.

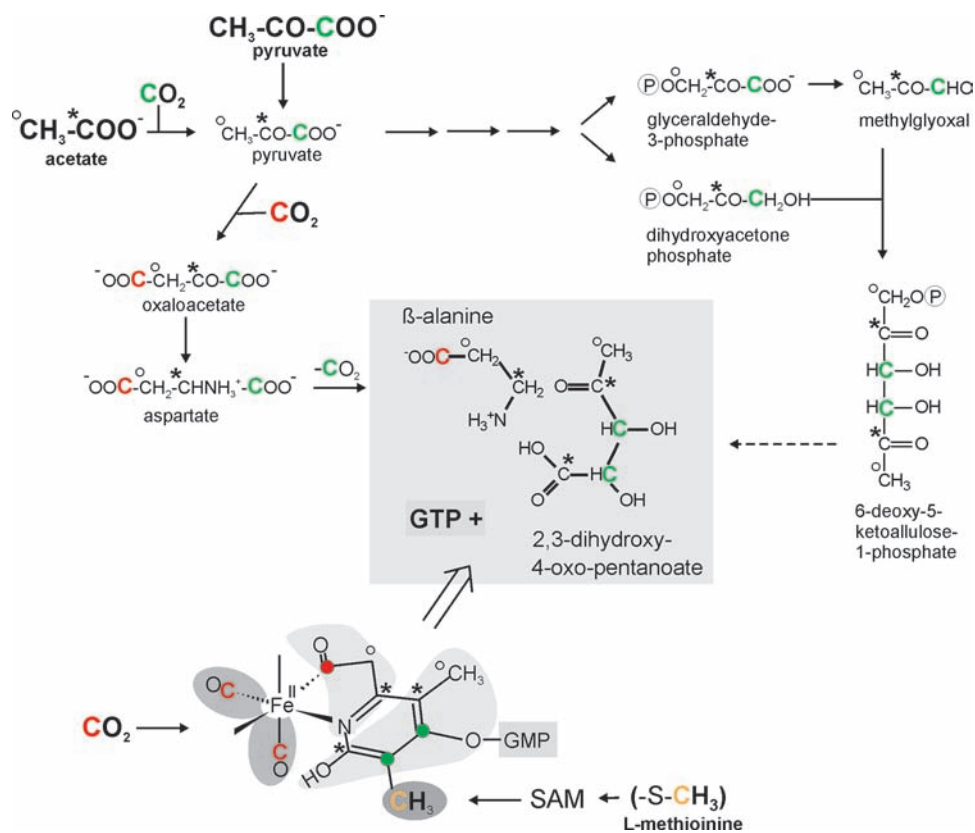


Figure 6. Putative biosynthetic pathway of the FeGP cofactor of [Fe]-hydrogenase from hydrogenotrophic methanogenic archaea as deduced from ¹³C labeling experiments. *Mt. marburgensis* or the acetate auxotrophic *Mb. smithii* were grown on H₂ and CO₂ as energy sources in the presence of [1-¹³C]acetate(*), [2-¹³C]acetate(°), [1-¹³C]pyruvate, ¹³CO₂, ¹³CO, or L-[methyl-²H₃]methionine. After harvest and isolation of the FeGP cofactor the labeling of the cofactor with ¹³C was determined via mass spectrometry and NMR. The labeling pattern was found to be consistent with a synthesis of the FeGP cofactor from one acetate, two pyruvate, three CO₂, and a methyl-group of methionine. Aspartate, 2,3-dihydroxy-4-oxo-pentanoate and S-adenosyl-methionine (SAM) are proposed intermediates although alternative pathways can be thought of. The formation of the pyridinol moiety from aspartate and the pentanoate could proceed via β -alanine as pyridoxal phosphate bound intermediate. The CO-ligands and the acyl carbon are exclusively derived from CO₂ but not via pyruvate C-1. In *Mb. smithii*, which is devoid of a nickel-dependent carbon monoxide dehydrogenase, CO₂ reduction to CO by the nickel enzyme is excluded. The unknown reaction(s) are indicated by arrows with a broken line. The predicted biochemical reactions in analogy to the retrosynthesis concept in organic chemistry are shown by the retrosynthesis arrow.

The putative intermediate 2,3-dihydroxy-4-oxo-pentanoate has a labeling pattern identical to that of the ribose moiety of the FeGP cofactor. This finding strongly suggested that a C₅ compound similar to ribose could be one of the precursors of pyridinol biosynthesis (Figure 6). Although 2,3-dihydroxy-4-oxo-pentanoate is not a known compound in methanogenic archaea, it could be synthesized involving known reactions such as the L-fucose-phosphate aldolase reaction in which methylglyoxal and dihydroxyacetone phosphate are condensed to 6-deoxy-5-ketoallulose-1-phosphate (Figure 6).³⁶ The isomer 6-deoxy-5-ketofructose-1-phosphate has been proposed to be an intermediate in aromatic amino acid biosynthesis in *Methanococcus maripaludis*.^{37,38} One of these C₆ compounds could be converted to the proposed C₅ intermediate via a series of enzyme reactions involving a phosphatase, a mutase, and an enzyme similar to hexulose-6-phosphate synthase to cleave the terminal hydroxyl methyl group. The C₅ product would have to be further converted in dehydrogenase reactions to form the carboxyl group. Alternatively the putative intermediate 2,3-dihydroxy-4-oxo-pentanoate could be synthesized via aldol condensation of methylglyoxal with glycolate or glycol aldehyde. Decarboxylation of aspartate yields the second putative intermediate β-alanine in the free or pyridoxal phosphate bound form, which has the same labeling pattern as the pyridinol ring at N(a), C(f), C(g), and C(h) (Figures 1 and 6). β-Alanine is an intermediate in the biosynthesis of coenzyme A in bacteria.³⁹ In the genome of archaea, a gene for aspartate decarboxylase is not found. However, the gene encoding the enzyme catalyzing pantothenate synthesis from β-alanine and pantoate is present.^{40,41}

In the biosynthesis of most pyridone-polyketides, the pyridinol moieties are produced from a polyketide chain and an amino acid, such as phenylalanine, tyrosine, serine, and β-alanine.^{42–44} The amino acid backbones are incorporated into the pyridone moiety at N(a), C(f), C(e), and C(d) (following the designation of the atoms of the iron-free FeGP cofactor). From the proposed biosynthetic pathway of pyridone-polyketides, the ¹³C-labeling pattern of their pyridinol ring, which was reconstructed from the biosynthetic pathway, is distinct from that of the FeGP cofactor. This shows that the biosynthetic precursors and reactions of the FeGP cofactor and pyridone-polyketides are not the same.

Genome analysis of methanogenic archaea has identified seven genes (*hcgA–G*) in addition to the [Fe]-hydrogenase structural gene *hmd* as a gene cluster that are predicted to be the FeGP cofactor biosynthesis genes.¹ The homology search revealed that one of the genes in the *hcg* gene cluster could be for radical-SAM-dependent enzyme (*hcgA*) and one for a SAM-dependent methyltransferase (*hcgG*). The *hcgA* gene shows high sequence similarity to that of biotin synthases and other radical-SAM-dependent enzymes.¹ However, HcgA lacks the CX₃CX₂C motif or CX₄CX₂C motif for [4Fe4S]-cluster that is characteristic of the N-terminal region for the radical-SAM protein superfamily and essential for radical formation.^{26,27} Instead, HcgA universally harbors a unique CX₅CX₂C motif.⁴⁵ The protein encoded by the *hcgG* gene is annotated as a fibrillar-like protein based on sequence similarity. Interestingly, the crystal structure of the C-terminal domain of the fibrillar homologue MJ0697 from *Methanocaldococcus jannaschii*⁴⁶ shows a similarity to the catalytic domain of SAM-dependent methyltransferases.⁴⁷ Sequence analysis of the *hcgB* gene product indicates that it may catalyze the ligation of the GMP and pyridinol parts of the cofactor. The crystal structure

of HcgB from *Mt. thermautotrophicum* has been determined (PDB code: 3BRC). The homodimeric protein shares structural similarities with a human inosine triphosphatase, which catalyzes cleavage of pyrophosphate from ITP.⁴⁸ The labeling pattern of the GMP part of the cofactor follows the canonical biosynthetic pathway also found in methanogenic archaea.

CONCLUSION

The stable-isotope-labeling experiments have set the frame in which the biosynthesis of the FeGP cofactor of [Fe]-hydrogenase in methanogenic archaea has to occur. The biosynthesis of the pyridinol moiety is definitely distinct from that of pyridone-polyketides. 2,3-Dihydroxy-4-oxo-pentanoate and β-alanine are discussed as intermediates to have at least a hypothesis of how the biosynthesis may occur and of what gene products could be involved. The C(j) methyl group attached to the pyridinol ring is derived from the methyl group of methionine and is most probably introduced via a SAM-dependent methyltransferase reaction. The CO ligands are synthesized from CO₂, but pyruvate C-1 does not appear to be involved indicating that the synthesis of the CO ligands in the FeGP cofactor differs from that in [FeFe]-hydrogenases. For the synthesis of the unique acyl–iron bond, the mechanism proposed for the formation of the acetyl–nickel bond in the catalytic cycle of acetyl-CoA synthase/decarbonylase is considered.

MATERIALS AND METHODS

Stable Isotopes. [1-¹³C]Acetate (99% ¹³C), [2-¹³C]acetate (99% ¹³C), [1-¹³C]glycine (99% ¹³C), [1-¹³C]propionate (99% ¹³C), L-[methyl-²H]methionine (99% ²H), [2,3-¹³C₂]succinate (99% ¹³C), and [1-¹³C]formate (99% ¹³C) were purchased from Euriso-tope. ¹³CO₂ (99% ¹³C) and ¹³CO (99% ¹³C) were from Sigma-Aldrich.

Growth of *Mt. marburgensis* and of *Mb. smithii*. *Mt. marburgensis* (DSM 2133) was grown at 65 °C in a mineral salt medium described by Schönheit et al.⁴⁹ For cultivation under nickel-limited conditions, the nickel concentration in the medium was decreased: in the 10 L fermenter, the nickel in the medium was omitted, and in the 500 mL glass fermenter and 2 L glass bottle cultures, the nickel concentration in the medium was lowered to 0.05 μM.¹⁵ For NMR sample preparation, *Mt. marburgensis* was cultivated in a 10 L fermenter with a continuous gas flow of H₂/CO₂ (80:20, vol/vol; 1.5 L/min). The ¹³C- or ²H-labeled compounds were added to the medium at the following final concentrations: 5 mM [2-¹³C]acetate, 5 mM [1-¹³C]acetate, 6.8 mM [1-¹³C]pyruvate, or 5 mM L-[methyl-²H]-methionine. For the electrospray ionization Fourier transform ion cyclotron resonance mass spectrometry (ESI-FT-ICR-MS) sample preparation, *Mt. marburgensis* was grown in the presence of 40 mM [1-¹³C]pyruvate, 5 mM [2,3-¹³C₂]succinate, or 40 mM [1-¹³C]formate in a 500 mL fermenter in 360 mL of medium with a continuous gas flow of H₂/CO₂ (80:20, vol/vol; 0.2 L/min); the pH of the medium was adjusted to 6.0 to facilitate the incorporation of the ¹³C-compounds.^{50,51} For ¹³C-incorporation from ¹³CO, *Mt. marburgensis* was batch cultivated in 500 mL of medium in 2 L glass bottles sealed with rubber stoppers under H₂/CO₂/¹³CO (80:20:2.5, by vol). The gas phase was exchanged three times during the daytime.

Mb. smithii (DSM 861) was grown at 37 °C under H₂/CO₂ (80:20, vol/vol) in a modified basal medium based on that of Balch et al.,⁵² in which sodium formate was omitted and the concentration of yeast extract was decreased from 2 g/L to 0.05 g/L. For the labeling, the medium contained 30 mM [1-¹³C]acetate, 30 mM [2-¹³C]acetate, 5 mM [1-¹³C]glycine, 2.5 mM [1-¹³C]propionate, or 2.5 mM L-[methyl-²H]methionine. For the ¹³CO₂ or ¹³CO incorporation experiments, the standard gas phase was substituted with H₂/¹³CO₂ (80:20, vol/vol) or H₂/CO₂/¹³CO (80:20:2.5, by vol).

Purification of the FeGP Cofactor from *Mt. marburgensis* and Generation of the Iron-Free FeGP Cofactor. [Fe]-hydrogenase was purified from 90 g of *Mt. marburgensis* cells by ammonium sulfate precipitation and anion-exchange chromatography as described previously.⁵³ The FeGP cofactor was extracted from the purified protein by 60% methanol/1 mM 2-mercaptoethanol/1% ammonia for 15 min at 40 °C under strictly anoxic conditions.⁵⁴ The cofactor preparation thus obtained was essentially homogeneous.

To obtain iron-free FeGP cofactor, 10 mL of cofactor preparation containing ~0.3 mM FeGP cofactor was placed on ice and exposed to high-intensity light (Cold Light Sources KL 2500 LC, Schott); the pH of the solution was then adjusted to 1–2. To completely remove the released iron ions, 0.6 mM EDTA (final concentration) was added to the light-exposed solution. The light decomposition product (iron-free FeGP cofactor) was purified by HPLC on a Synergi 4 m Polar RP 80A column (250 mm × 4.6 mm) using a linear H₂O/CH₃OH gradient. The purified iron-free FeGP cofactor was dried by evaporation at 4 °C and then dissolved in 200 μL of D₂O prior to NMR measurements.

Purification of the FeGP Cofactor from *Mb. smithii*. [Fe]-hydrogenase was partially purified from *Mb. smithii* cells under strictly anoxic conditions under red light. The cells (2–3 g fresh weight) were harvested at the end of the exponential growth phase by centrifugation (16 000 × g for 30 min at 4 °C) and suspended in 5 mL of 50 mM phosphate buffer, pH 7.0. The cells were disrupted on ice by ultrasonication (Sonopuls GM200, Ti73 tip, Bandelin) for 15 min with 50% cycle and 60% power. The cell extract exhibited 0.03 U/mg [Fe]-hydrogenase activity (Figure S7, Supporting Information). After centrifugation (16 000 × g for 30 min at 4 °C), the soluble fraction was separated from the membrane fraction by ultracentrifugation (140 000 × g for 30 min at 4 °C). Ammonium sulfate powder was added to 60% saturation to the supernatant on ice, and the precipitated proteins were removed by centrifugation at 13 000 × g for 15 min at 4 °C. The [Fe]-hydrogenase fraction was precipitated by adding ammonium sulfate to 90% saturation to the supernatant. After centrifugation (16 000 × g for 30 min at 4 °C), the precipitate was dissolved in anoxic water and desalted using an ultrafilter (30-kDa cutoff). The FeGP cofactor was extracted either in 60% methanol/1 mM 2-mercaptoethanol/1% ammonia for MALDI-TOF-MS or in 50% acetic acid for ESI-FT-ICR-MS, as described previously.¹⁰ The FeGP cofactor was separated from the unfolded proteins by ultrafiltration (5-kDa cutoff) before mass spectrometry.

Mass Spectrometry and NMR Spectroscopy. The FeGP cofactor was analyzed by MALDI-TOF-MS using a 4800 Proteomics Analyzer (Applied Biosystems/MDS Sciex) with α -cyano-4-hydroxycinnamic acid dissolved in 70% (v/v) acetonitrile and 0.1% (v/v) trifluoroacetic acid as matrix. The cofactor was analyzed by ESI-FT-ICR mass spectrometry using an LTQ-FT-Ultra (Thermo Scientific) equipped with HPLC (Macherey-Nagel 125/2 Nucleodur C18ec column and water/methanol as solvents). For NMR, about 0.5 mg of the iron-free cofactors with various labeling patterns were dissolved in 200 μL of ²H₂O and filled into Wilmad 3 mm NMR tubes (Rototec Spintec). Two-dimensional (2D) experiments were performed on a Bruker AV600 spectrometer with a TXI ¹H–¹³C/¹⁵N probe installed with z-gradient, while ¹³C and ³¹P spectra were recorded on a Bruker AV500 spectrometer with broadband forward probe BBFO. The one-dimensional (1D) spectra, ¹H, ¹³C, and ³¹P, and the 2D spectra, ¹H–¹³C HSQC and HMBC spectra, were recorded with standard pulse programs at 300 K.⁵⁵ The 1D spectra were acquired with 65 536 data points, while 2D spectra were collected using 2048 points in the F₂ dimension and 512 increments in the F₁ dimension. For the HSQC spectra, 32–64 transients, for the HMBC 64–128 transients, for ¹H 128–1024, and for ¹³C 24576–92160 scans were used. The relaxation delay was 3.0 s. Chemical shifts of ¹H and ¹³C spectra were referenced to the signals of 4,4-dimethyl-4-silapentane sodium sulfonate. The spectra were processed by Bruker Topspin 3.0.

Infrared Spectroscopy. Attenuated total reflection infrared (ATR-IR) spectroscopy was performed using a Bruker Vertex 70 FTIR spectrometer equipped with an MCT detector. ATR optical configuration (DuraSampler, SensIR Technologies) was employed with a silicon prism.⁵⁶

Protein and Enzyme Activity Assays. The protein concentration was determined by the Bradford method using the assay solution from Bio-Rad and bovine serum albumin as the standard. The enzyme activity of [Fe]-hydrogenase purified from methanogens and of that reconstituted from the isolated FeGP cofactor and the apoenzyme heterologously produced in *Escherichia coli* were assayed as described previously.⁵³

■ ASSOCIATED CONTENT

📄 Supporting Information

Standard ¹³C NMR spectra of the ¹³C-labeled iron-free FeGP cofactor with various labeling patterns, ¹H–¹³C HMBC of iron-free FeGP cofactor labeled with ¹³C from [2-¹³C]acetate, ¹H NMR spectrum of iron-free FeGP cofactor labeled with ²H from L-[methyl-²H₃]methionine, simulation of the isotopic profiles of the mass spectra, MALDI-TOF-MS of the FeGP cofactor detected in the cell extract of *Mb. smithii* cultivated in the presence of 2.5 mM [1-¹³C]propionate, MALDI-TOF-MS spectrum of the FeGP cofactor detected in the cell extract of *Mt. marburgensis* cultivated in the presence of 5 mM [2,3-¹³C₂]succinate, and [Fe]-hydrogenase activity in cell extract of *Mb. smithii*. This material is available free of charge via the Internet at <http://pubs.acs.org>.

■ AUTHOR INFORMATION

Corresponding Author

shima@mpi-marburg.mpg.de

Notes

The authors declare no competing financial interest.

■ ACKNOWLEDGMENTS

This work was supported by a grant of the Max Planck Society to R. K. Thauer, by a grant of the PRESTO program, Japan Science and Technology Agency (JST), to S. Shima and by the BMBF BioH₂ project. We thank W. Buckel (Philipps University Marburg) for discussions on the reaction mechanism and R. K. Thauer for many helpful suggestions including the critical reading of the manuscript. Also the technical assistance of Jan Bamberger during ESI-MS measurements is acknowledged.

■ REFERENCES

- (1) Thauer, R. K.; Kaster, A. K.; Goenrich, M.; Schick, M.; Hiromoto, T.; Shima, S. *Annu. Rev. Biochem.* **2010**, *79*, 507.
- (2) DiMarco, A. A.; Bobik, T. A.; Wolfe, R. S. *Annu. Rev. Biochem.* **1990**, *59*, 355.
- (3) Zirngibl, C.; van Dongen, W.; Schwörer, B.; von Büna, R.; Richter, M.; Klein, A.; Thauer, R. K. *Eur. J. Biochem.* **1992**, *208*, 511.
- (4) Hiromoto, T.; Ataka, K.; Pilak, O.; Vogt, S.; Stagni, M. S.; Meyer-Klaucke, W.; Warkentin, E.; Thauer, R. K.; Shima, S.; Ermler, U. *FEBS Lett.* **2009**, *583*, 585.
- (5) Hiromoto, T.; Warkentin, E.; Moll, J.; Ermler, U.; Shima, S. *Angew. Chem., Int. Ed.* **2009**, *48*, 6457.
- (6) Korbas, M.; Vogt, S.; Meyer-Klaucke, W.; Bill, E.; Lyon, E. J.; Thauer, R. K.; Shima, S. *J. Biol. Chem.* **2006**, *281*, 30804.
- (7) Lyon, E. J.; Shima, S.; Boecher, R.; Thauer, R. K.; Grevels, F. W.; Bill, E.; Roseboom, W.; Albracht, S. P. J. *J. Am. Chem. Soc.* **2004**, *126*, 14239.
- (8) Salomone-Stagni, M.; Stellato, F.; Whaley, C. M.; Vogt, S.; Morante, S.; Shima, S.; Rauchfuss, T. B.; Meyer-Klaucke, W. *Dalton Trans.* **2010**, *39*, 3057.
- (9) Shima, S.; Lyon, E. J.; Thauer, R. K.; Mienert, B.; Bill, E. *J. Am. Chem. Soc.* **2005**, *127*, 10430.
- (10) Shima, S.; Schick, M.; Ataka, K.; Steinbach, K.; Linne, U. *Dalton Trans.* **2012**, *41*, 767.

- (11) Henry, T. A. *Plant Alkaloids*, 4th ed.; The Blakiston Company: Philadelphia, PA, 1949.
- (12) Shima, S.; Pilak, O.; Vogt, S.; Schick, M.; Stagni, M. S.; Meyer-Klaucke, W.; Warkentin, E.; Thauer, R. K.; Ermler, U. *Science* **2008**, *321*, 572.
- (13) Yang, X. Z.; Hall, M. B. *J. Am. Chem. Soc.* **2009**, *131*, 10901.
- (14) Dent, S. P.; Eaborn, C.; Pidcock, A.; Ratcliff, B. *J. Organomet. Chem.* **1972**, *46*, C68.
- (15) Afting, C.; Hochheimer, A.; Thauer, R. K. *Arch. Microbiol.* **1998**, *169*, 206.
- (16) Kaster, A. K.; Goenrich, M.; Seedorf, H.; Liesegang, H.; Wollherr, A.; Gottschalk, G.; Thauer, R. K. *Archaea* **2011**, *2011*, No. 973848.
- (17) Samuel, B. S.; Hansen, E. E.; Manchester, J. K.; Coutinho, P. M.; Henrissat, B.; Fulton, R.; Latreille, P.; Kim, K.; Wilson, R. K.; Gordon, J. I. *Proc. Natl. Acad. Sci. U.S.A.* **2007**, *104*, 10643.
- (18) Shima, S.; Lyon, E. J.; Sordel-Klippert, M. S.; Kauss, M.; Kahnt, J.; Thauer, R. K.; Steinbach, K.; Xie, X. L.; Verdier, L.; Griesinger, C. *Angew. Chem., Int. Ed.* **2004**, *43*, 2547.
- (19) Choquet, C. G.; Richards, J. C.; Patel, G. B.; Sprott, G. D. *Arch. Microbiol.* **1994**, *161*, 471.
- (20) Vogt, S. Doctor thesis, Philipps University, 2007.
- (21) Kang, Y. N.; Tran, A.; White, R. H.; Ealick, S. E. *Biochemistry* **2007**, *46*, 5050.
- (22) Angelaccio, S.; Chiaraluce, R.; Consalvi, V.; Buchenau, B.; Giangiacomo, L.; Bossa, F.; Contestabile, R. *J. Biol. Chem.* **2003**, *278*, 41789.
- (23) Choquet, C. G.; Richards, J. C.; Patel, G. B.; Sprott, G. D. *Arch. Microbiol.* **1994**, *161*, 481.
- (24) Goenrich, M.; Thauer, R. K.; Yurimoto, H.; Kato, N. *Arch. Microbiol.* **2005**, *184*, 41.
- (25) Schröder, I.; Thauer, R. K. *Eur. J. Biochem.* **1999**, *263*, 789.
- (26) Buckel, W.; Thauer, R. K. *Angew. Chem., Int. Ed.* **2011**, *50*, 10492.
- (27) Zhang, Q.; van der Donk, W. A.; Liu, W. *Acc. Chem. Res.* **2012**, DOI: 10.1021/ar200202c.
- (28) Shepard, E. M.; Duffus, B. R.; George, S. J.; McGlynn, S. E.; Challand, M. R.; Swanson, K. D.; Roach, P. L.; Cramer, S. P.; Peters, J. W.; Broderick, J. B. *J. Am. Chem. Soc.* **2010**, *132*, 9247.
- (29) Swanson, K. D.; Duffus, B. R.; Beard, T. E.; Peters, J. W.; Broderick, J. B. *Eur. J. Inorg. Chem.* **2011**, *2011*, 935.
- (30) Burstel, I.; Hummel, P.; Siebert, E.; Wisitruangsakul, N.; Zebger, I.; Friedrich, B.; Lenz, O. *J. Biol. Chem.* **2011**, *286*, 44937.
- (31) Chen, D.; Scopelliti, R.; Hu, X. *Angew. Chem., Int. Ed.* **2010**, *49*, 7512.
- (32) Chen, D. F.; Scopelliti, R.; Hu, X. L. *Angew. Chem., Int. Ed.* **2011**, *50*, 5671.
- (33) Ragsdale, S. W. *J. Inorg. Biochem.* **2007**, *101*, 1657.
- (34) Tan, X. S.; Surovtsev, I. V.; Lindahl, P. A. *J. Am. Chem. Soc.* **2006**, *128*, 12331.
- (35) Bacher, A.; Rieder, C.; Eichinger, D.; Arigoni, D.; Fuchs, G.; Eisenreich, W. *FEMS Microbiol. Rev.* **1998**, *22*, 567.
- (36) Grochowski, L. L.; Xu, H. M.; White, R. H. *J. Bacteriol.* **2006**, *188*, 2836.
- (37) Porat, I.; Sieprawska-Lupa, M.; Teng, Q.; Bohanon, F. J.; White, R. H.; Whitman, W. B. *Mol. Microbiol.* **2006**, *62*, 1117.
- (38) White, R. H. *Biochemistry* **2004**, *43*, 7618.
- (39) Begley, T. P.; Kinsland, C.; Strauss, E. *Vitam. Horm.* **2001**, *61*, 157.
- (40) Genschel, U. *Mol. Biol. Evol.* **2004**, *21*, 1242.
- (41) Ronconi, S.; Jonczyk, R.; Genschel, U. *FEBS J.* **2008**, *275*, 2754.
- (42) Fujita, Y.; Oguri, H.; Oikawa, H. *Tetrahedron Lett.* **2005**, *46*, 5885.
- (43) Weber, T.; Laiple, K. J.; Pross, E. K.; Textor, A.; Grond, S.; Welzel, K.; Pelzer, S.; Vente, A.; Wohlleben, W. *Chem. Biol.* **2008**, *15*, 175.
- (44) Eley, K. L.; Halo, L. M.; Song, Z.; Powles, H.; Cox, R. J.; Bailey, A. M.; Lazarus, C. M.; Simpson, T. J. *ChemBioChem* **2007**, *8*, 289.
- (45) McGlynn, S. E.; Boyd, E. S.; Shepard, E. M.; Lange, R. K.; Gerlach, R.; Broderick, J. B.; Peters, J. W. *J. Bacteriol.* **2010**, *192*, 595.
- (46) Wang, H. M.; Boisvert, D.; Kim, K. K.; Kim, R.; Kim, S. H. *EMBO J.* **2000**, *19*, 317.
- (47) Sankpal, U. T.; Rao, D. N. *Crit. Rev. Biochem. Mol. Biol.* **2002**, *37*, 167.
- (48) Stenmark, P.; Kursula, P.; Flodin, S.; Graslund, S.; Landry, R.; Nordlund, P.; Schuler, H. *J. Biol. Chem.* **2007**, *282*, 3182.
- (49) Schönheit, P.; Moll, J.; Thauer, R. K. *Arch. Microbiol.* **1980**, *127*, 59.
- (50) Huster, R.; Thauer, R. K. *FEMS Microbiol. Lett.* **1983**, *19*, 207.
- (51) Diekert, G.; Gilles, H. H.; Jaenchen, R.; Thauer, R. K. *Arch. Microbiol.* **1980**, *128*, 256.
- (52) Balch, W. E.; Fox, G. E.; Magrum, L. J.; Woese, C. R.; Wolfe, R. S. *Microbiol. Rev.* **1979**, *43*, 260.
- (53) Shima, S.; Schick, M.; Tamura, H. *Methods Enzymol.* **2011**, *494*, 119.
- (54) Lyon, E. J.; Shima, S.; Buurman, G.; Chowdhuri, S.; Batschauer, A.; Steinbach, K.; Thauer, R. K. *Eur. J. Biochem.* **2004**, *271*, 195.
- (55) Berger, S.; Braun, S. *200 and More NMR experiments, a practical course*; Wiley-VCH: Weinheim, Germany, 2004.
- (56) Shima, S.; Ataka, K. *FEBS Lett.* **2011**, *585*, 353.